ICSV13 - Vienna
The Thirteenth International Congress on Sound and Vibration
Vienna, Austria, July 2-6, 2006

# USE OF A COUPLED MECHANICAL-ACOUSTIC COMPUTATIONAL MODEL TO IDENTIFY FAILURE MECHANISMS IN PAPER PRODUCTION

David Kao*[1], Koulis Pericleous*[1], Deryn Graham[1] and Brian Knight[1]

[1]School of Computing and Mathematical Sciences, University of Greenwich, Park Row
Greenwich, London, SE10 9LS
d.kao@gre.ac.uk
k.pericleous@gre.ac.uk

## Abstract

In this paper, a coupled mechanical-acoustic system of equations is solved to determine the relationship between emitted sound and damage mechanisms in paper under controlled stress conditions. The simple classical expression describing the frequency of a plucked string to its material properties is used to generate a numerical representation of the microscopic structure of the paper, and the resulting numerical model is then used to simulate the vibration of a range of simple fibre structures when undergoing two distinct types of damage mechanisms: (a) fibre/fibre bond failure, (b) fibre failure. The numerical results are analysed to determine whether there is any detectable systematic difference between the resulting acoustic emissions of the two damage processes. Fourier techniques and are then used to compare the computed results against experimental measurements. Distinct frequency components identifying each type of damage are shown to exist, and in this respect theory and experiments show good correspondence. Hence, it is shown, that although the mathematical model represents a grossly-simplified view of the complex structure of the paper, it nevertheless provides a good understanding of the underlying micro-mechanisms characterising its properties as a stress-resisting structure. Use of the model and accompanying software will enable operators to identify approaching failure conditions in the continuous production of paper from emitted sound signals and take preventative action.

## INTRODUCTION

This paper will present a method for distinguishing between the fibre/fibre bond failure and fibre failure damage mechanisms present in the paper fibre structure using a hybrid vibro-acoustic model. The vibro-acoustic model is a coupling of two well-known systems, the mass/spring paradigm [1], [2] and the acoustic wave equation [4, 13], and will be used to simulate the acoustic response of several simple fibre structures undergoing different failure types.

The results obtained from the numerical model are then analysed using the continuous wavelet transform (CWT) [3, 7, 12] to provide a time/frequency representation of the acoustic signal. The CWT provides critical temporal information on the different frequency components of the acoustic emission (AE), which establishes suitable criteria for the identification of the two damage mechanisms. The software to calculate the CWT is provided by Vallen-Systeme [11].

## THE VIBRO-ACOUSTIC MODEL

The vibro-acoustic model employs the mass/spring model to simulate the movement of the fibre structure as shown by Equation 1.

$$m_i \frac{d^2\mathbf{r}_i}{dt^2} + \sum_j k_{ij}(||\mathbf{r}_j - \mathbf{r}_i|| - L_{i,j}) \frac{\mathbf{r}_j - \mathbf{r}_i}{||\mathbf{r}_j - \mathbf{r}_i||} + b_i \frac{d\mathbf{r}_i}{dt} = 0 \qquad (1)$$

where $\mathbf{r}$ is the mass position vector, $m_i$ is the mass of mass $i$, $b_i$ is the damping constant on mass $i$ and $k_{ij}$ is the stiffness and $L_{ij}$ is the original length of the spring connecting masses $i$ and $j$.

The movement from the mass/spring model is coupled to the acoustic pressure wave equation as shown in Equation 2 by means of Equation 3.

$$\frac{\partial^2 p}{\partial t^2} = c^2 \left( \nabla^2 p - \nabla \cdot \mathbf{F} + \rho \frac{\partial q}{\partial t} \right) \qquad (2)$$

$$\frac{\partial q}{\partial t} = \frac{d\mathbf{u}_{ms}}{dt} \qquad (3)$$

where $p$ is the acoustic pressure, $c$ is the speed of sound in the medium, $\mathbf{F}$ is an external force, $\rho \frac{\partial q}{\partial t}$ is known as the volumetric acceleration and $\mathbf{u}_{\mathrm{ms}}$ is the velocity vector of the masses from the mass/spring model. The numerical model can now be used to simulate the damage mechanisms in paper using several simple fibre structures, but first it is prudent to discuss the numerical implementation of the vibro-acoustic model.

## NUMERICAL IMPLEMENTATION

The mass/spring model is solved using a first order implicit Euler method, which has the advantage of being unconditionally stable irrespective of the time step. The system of equations to be solved, as derived by Baraff *et al* [1], is shown in Equation 4.

$$\left(I + \Delta t M^{-1}\frac{\partial \mathbf{f}^n}{\partial \mathbf{u}} + \Delta t^2 M^{-1}\frac{\partial \mathbf{f}^n}{\partial \mathbf{r}}\right)\Delta \mathbf{u} = -\Delta t M^{-1}\left(\mathbf{f}^n + \Delta t \frac{\partial \mathbf{f}^n}{\partial \mathbf{r}}\mathbf{u}^n\right) \qquad (4)$$

where $I$ is the identity matrix, $M^{-1}$ is the inverse mass matrix and **f** is defined by Equation 5.

$$\mathbf{f}_i^n = \sum_j k_{ij}\left(1 - \frac{L_{ij}}{||\mathbf{r}_j^n - \mathbf{r}_i^n||}\right)(\mathbf{r}_j^n - \mathbf{r}_i^n) + b_i \mathbf{u}_i^n \qquad (5)$$

The mass/spring model is solved using the BiConjugate Gradient Method, as described by Press *et al* [9], as the matrix in Equation 4 is non-symmetric. The acoustic wave equation is discretised using a fourth order accurate central differencing scheme for the spatial components and a second order accurate central differencing scheme for the temporal component as stated by Zakaria *et al* [13] and can be seen in Equation 6.

$$\begin{aligned} p_{i,j}^{k+1} = (2 - 5\alpha^2)p_{i,j}^k - p_{i,j}^{k-1} + \frac{4}{3}\alpha^2\left(p_{i+1,j}^k + p_{i-1,j}^k + p_{i,j+1}^k + p_{i,j-1}^k\right) \\ -\frac{1}{12}\alpha^2\left(p_{i+2,j}^k + p_{i-2,j}^k + p_{i,j+2}^k + p_{i,j-2}^k\right) \end{aligned} \qquad (6)$$

where $\alpha = \frac{c\Delta t}{\Delta h}$, $\Delta t$ is the time step, $\Delta h$ is the cell width/height, $i,j$ position in space and $k$ is the position in time. The acoustic wave equation is solved using an explicit Gauss-Siedel method. The numerical algorithm is implemented in JAVA and Table 1 lists the simulation information for the two damage mechanisms when run on an AMD Athlon 64 3200+ with 512MB running Gentoo Linux.

*Table 1 – Simulation Information*

| | *Fibre/Fibre Bond Failure* | *Fibre Failure* |
|---|---|---|
| *Preliminary Iterations* | 100000 | 100000 |
| *Mass/Spring Iterations* | 4000 | 4000 |
| *Acoustic Wave Iterations* | 400 | 400 |
| *Number of Masses* | 165 | 84 |
| *Number of Springs* | 168 | 83 |
| *Time Taken* | 5210.30 s | 738.08 s |

The large disparity in the time taken for the two simulations, as shown in Table 1, is due to the requirement that the sparse matrix (the left hand side of Equation 4) must be populated every iteration. An increase in the number of masses produces a non-linear increase in the total time taken.

## THE CLASSICAL STRING

The frequency produced by a vibrating string is dependent on the tension within the string and the linear density of the string as stated by Rossing [10]. In terms of the mass/spring model it leads to the following relationship.

$$F \propto \frac{kx}{m} \quad \text{where:} \quad k = \frac{Etw}{L} \tag{7}$$

In terms of the fundamental properties of a fibre, Equation 7 becomes.

$$F \propto \frac{Etwx}{Lm} \tag{8}$$

where *E* is the Young's Modulus, *t* is the thickness, *w* is the width, *L* is the free vibrating length and *m* is the mass of the paper fibre and *x* is the displacement of the paper fibre from equilibrium. Using Equation 8 it is possible to predict how the changes in the fibre structure due to the two damage mechanisms affect its frequency of vibration. The following section will address the assumptions associated with Equation 8.

## ASSUMPTIONS OF THE FIBRE STRUCTURE

To successfully model the acoustic response of the two damage mechanisms, several assumptions regarding the fibre structure and individual fibre properties must be properly addressed.

### Free Vibrating Length

Figure 1 shows a typical notched paper sample stressed at 98% of its failure load. The two opaque regions located next to each notch show the area of the paper that has already undergone significant damage. More importantly, it shows that the length of the damage zone is no more than 1 mm in length. Therefore it is assumed that the fibre structure outside of the damage zone remains in its virgin state. If no deformation has occurred then the fibre structure outside of the damage zone can be thought of as having an infinite mass. This leads to the first assumption that the free vibrating length of a paper fibre in the damage zone is equal to 1 mm.

### Extension of the Paper Fibre

Figure 2 shows the extension of the paper specimen versus the AE number. The paper sample has a length of 100 mm and undergoes a maximum extension of 0.85 mm. This equates to approximately 1% of the length of the paper sample. For simplicity, it is assumed that the internal structure of the paper is a Cartesian mesh of fibre so that an extension of 1 % in the macroscopic length of the paper is equal to an extension of 1% in each fibre.

**Material Properties of the Paper Fibre**

The previous two sections have dealt with the variables $L$ and $x$ from Equation 8. The remainder of the material properties are average values as stated by Gregerson [6].

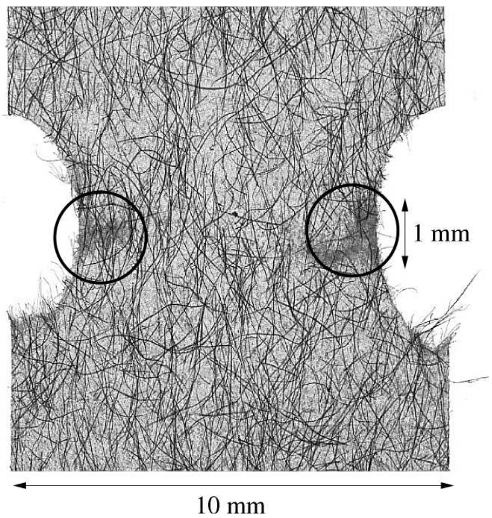


*Figure 1 – Sample Showing the Size of the Damage Zone in the Paper*

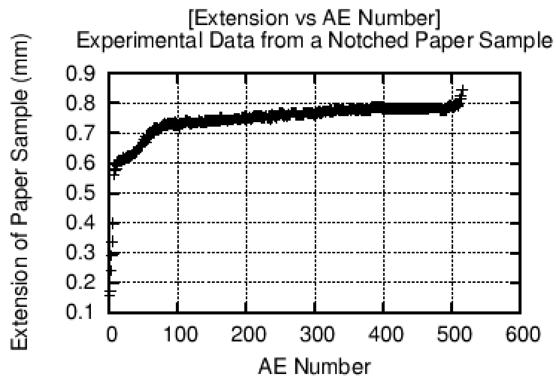


*Figure 2 – Extension of a Typical Paper Fibre*

## THE NUMERICAL RESULTS

This paper will present results on two simple fibre structures, the first will simulate the fibre/fibre bond failure damage mechanism and the second will simulate the fibre failure damage mechanism.

**The Fibre/Fibre Bond Failure Damage Mechanism**

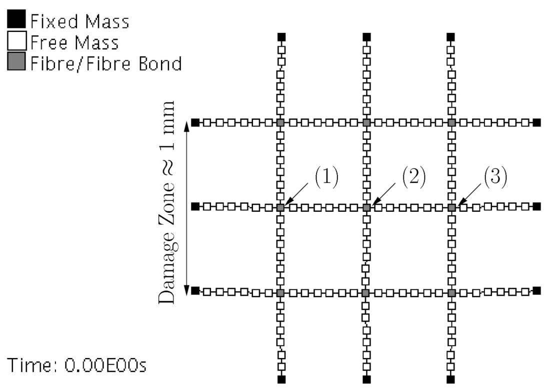


*Figure 3 – 3x3 Cartesian Mesh showing Potential Fibre/Fibre Bond Failures*

The fibre/fibre bonds present in the paper structure are weaker than the fibres themselves and as such are more likely to fail before any fibres. To represent an undamaged fibre structure, a 3x3 Cartesian mesh is used as shown in Figure 3.

Figure 4 shows the CWT of the AE generated when fibre/fibre bond (1) fails, with Figure 5 showing the CWT from a typical experimental fibre/fibre bond failure. The experimental results are obtained from a tensile test for a notched paper specimen as stated by Graham *et al* [5]. It is clear from the theoretical and experimental results that the *fibre/fibre bond failure* has two dominant frequency components at approximately 250 kHz and 750 kHz. It is also important to note that the shapes of the two CWTs are similar.

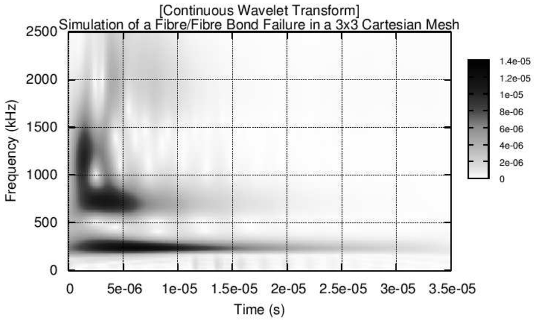


*Figure 4 – Theoretical Fibre/Fibre Bond Failure*

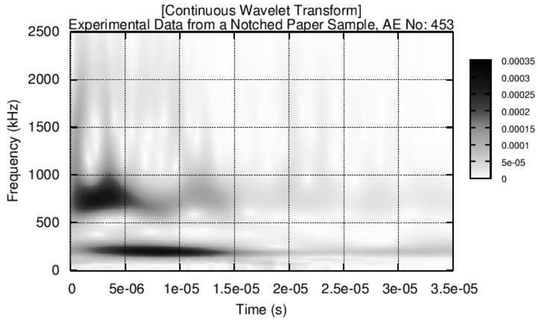


*Figure 5 – Experimental Fibre/Fibre Bond Failure*

**The Fibre Failure Damage Mechanism**

To represent the *fibre failure* damage mechanism, it is assumed that all bonds within the damage zone have failed. Certain fibres from the 3x3 Cartesian mesh were omitted from this structure to represent the absence of fibre/fibre bonds in the damage zone. This 2x1 fibre structure can be seen in Figure 6.

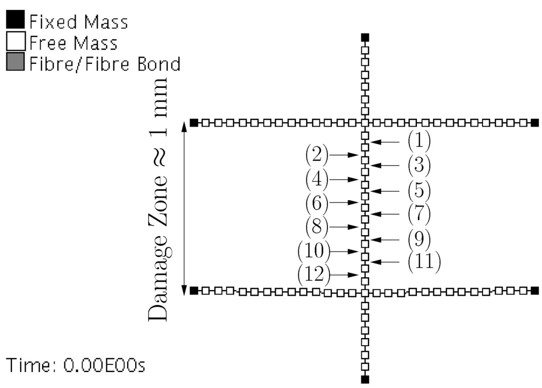


*Figure 6 – 2x1 Fibre Structure showing Potential Fibre Failure Points*

Figure 7 shows the CWT of the AE generated when the fibre fails at point (7), with Figure 8 showing the CWT of a typical experimental fibre failure. It is clear from the theoretical and experimental results that a fibre failure has a strong, but fleeting high frequency component at the beginning of the signal.

From Figures 4 and 7 it is possible to define criteria from the CWTs for identifying the two damage mechanisms. The criteria for a fibre/fibre bond failure are listed below.

- The dominant frequency components of the AE must be at approximately 250 kHz or 750 kHz.
- The strongest frequency component may be at either approximately 250 kHz or 750 kHz.
- The duration of the frequency component at approximately 250 kHz is longer than that of the frequency component at approximately 750 kHz.

Finally, the criteria for identifying a fibre failure are given below.

- The dominant frequency component of the AE must be greater than 800 kHz
- The duration of the dominant frequency component must be less than 5.00E-06 seconds.
- The dominant frequency component must be present at the front of the AE.

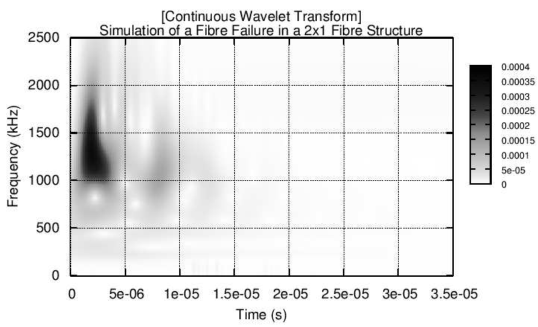


*Figure 7 – Theoretical Fibre Failure*

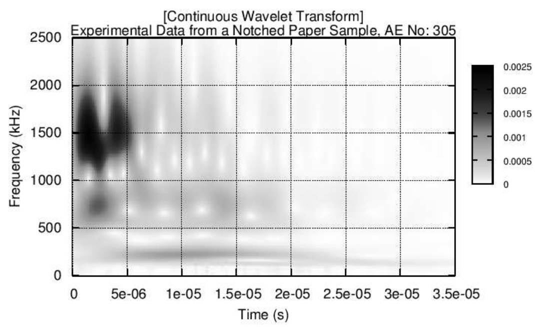


*Figure 8 – Experimental Fibre Failure*

## CONCLUSIONS

This work has developed a numerical model which is able to provide an understanding of the micro-mechanics of the paper structure through the use of AEs by simulating the movement of simplistic fibre structures. The model is not limited to simple structures and can be used to reproduce an actual fibre mesh by copying a micrograph of paper or by generating a random mesh.

The fibre/fibre bond failure and fibre failure damage mechanisms are successfully modelled to produce a theoretical time/frequency representation of the resulting AE. The differences in the CWTs of the two damage mechanisms show that the fibre/fibre bond failure results in a low frequency wave and the fibre failure results in a high frequency pulse. The time and frequency values as specified by the above criteria are dependent on the material properties of the paper fibres, as shown by Equation 4, but the shape of the CWTs is intrinsic to the physics of the damage mechanisms and should be present in any paper type. This result enables the dynamic identification of AEs during an experimental test and with further research can provide a gauge for the onset of fracture for a range of paper types. The paper used in this experiment is made from hand beaten chemical pulp as specified by Nyström [8].

## ACKNOWLEDGEMENTS

This work is funded by the European Union project QLK5-CT-2002-00772 AEP, a European Union Fifth Frame Program.

## REFERENCES

[1] D. Baraff, A. Witkin, "Large steps in cloth simulation", In Computer Graphics, 43-45, SIGGRAPH (1998)

[2] K-J. Choi, H-S. Ko, "Stable but responsive cloth", In ACM Transactions on Graphics, 604-611, SIGGRAPH (2002)

[3] C. K. Chui, *An Introduction to Wavelets.* (Academic Press, 1992)

[4] F. J. Fahy, *Sound Intensity.* (E & F N Spon, 1995)

[5] D. Graham, D. Kao, B. Knight, P. Gradin, P. Isaksson, S. Nyström, "Acoustic emission applied to mechanically loaded paper", In 26th Conference on Acoustic Emission Testing, EWGAE (2004)

[6] Ø. Gregerson, "Material properties of paper", Personal Communication, 2005

[7] G. Kaiser, *A Friendly Guide to Wavelets.* (Birkhäuser, 1994)

[8] S. Nyström, "Tensile Paper Test with a 2 Sensor Array", Experimental Data 2005-02-01, AEP QLK5-CT-2002-00772

[9] W. H. Press, S. A. Teukolsky, W. T. Vetterling, B. P. Flannery, *Numerical Recipes in C++, The Art of Scientific Computing.* (Cambridge University Press, 2002)

[10] T. D. Rossing, N. H. Fletcher, *Principles of Sound and Vibration.* (Springer-Verlag, 1995)

[11] H. Vallen, J. Vallen, "Free-of-cost software tools generate dispersion curves, perform wavelet transform and help correlate both kinds of information", Technical Report, Vallen-Systeme

[12] R. K. Young, *Wavelet Theory and its Applications.* (Kluwer Academic, 1993)

[13] A. Zakaria, J. Penrose, F. Thomas, X. Wang, "The two dimensional numerical modelling of acoustic wave propagation in shallow water", Acoustics (2000)